Chowarit Mitsantisuk, Manuel Nandayapa, Kiyoshi Ohishi, Seiichiro Katsura

Design for Sensorless Force Control of Flexible Robot by Using Resonance Ratio Control Based on Coefficient Diagram Method

Original scientific paper

Generally, the flexible robot system can be modeled as the two-mass system which consists of a motor and load connected by a spring. Thus, its elasticity causes resonance in the system. By using the conventional PID controller, this method cannot perform well in this situation. Much research has proceeded with the aim of reducing vibration. A new effective control method, the resonance ratio control, has been introduced as a new way to guarantee the robustness and suppress the oscillation during task executions for a position and force control. In this paper, three techniques are proposed for improving the performance of resonance ratio control. Firstly, a new multi encoder based disturbance observer (MEDOB) is shown to estimate the disturbance force on the load side. The proposed observer is not necessary to identify the nominal spring coefficient. Secondly, coefficient diagram method (CDM) has been applied to calculate a new gain of the force controller. A new resonance ratio gain has been presented as 2.0. Finally, the MEDOB and load side disturbance observer (LDOB) are employed to identify a spring coefficient of flexible robot system. By using the proposed identification method, it is simple to identify the spring coefficient and easy to implement in the real flexible robot system. The effectiveness of the proposed identification method is verified by simulation and experimental results.

Key words: Disturbance observer, Two-mass system, Coefficient diagram method, Resonance ratio control

Sinteza bezsenzornog upravljanja silom za fleksibilnog robota korištenjem upravljanja omjerom rezonancija temeljenim na metodi koeficijentnog dijagrama. Općenito, sustav fleksibilnog robota može se modelirati kao dvomaseni sustav koji se sastoji od motora i tereta povezanih oprugom. Rezonancija sustava posljedica je elastičnosti opruge. Korištenje konvencionalnog PID regulatora ne daje zadovoljavajuće performanse u ovoj situaciji. Provedena su mnoga istraživanja s ciljem smanjenja vibracija. Tako je uvedena nova učinkovita metoda upravljanja, upravljanje omjerom rezonancija, kao novi način da se osigura robusnost i priguše oscilacije tijekom izvršavanja zadatka putem upravljanja pozicijom i silom. U ovom radu predložene su tri tehnike za poboljšanje performansi upravljanja omjerom rezonancija. Prvo, pokazano je kako novi observer poremećaja temeljen na više enkodera (MEDOB) estimira poremećajnu silu na strani tereta. Predloženi observer nije nužan za identifikaciju nominalnog koeficijenta opruge. Drugo, metoda koeficijentnog dijagrama (CDM) je primijenjena za proračun novog pojačanja regulatora sile. Iznos 2.0 je određen kao novo pojačanje omjera rezonancija. Konačno, MEDOB i observer poremećaja na strani tereta (LDOB) korišteni su za identifikaciju koeficijenta opruge sustava fleksibilnog robota. Predložena metoda identifikacije jednostavna je za implementaciju na stvarni sustav, te se pomoću nje jednostavno identificira koeficijent opruge. Učinkovitost predložene metode identifikacije provjerena je simulacijski i eksperimentalno.

Ključne riječi: observer poremećaja, dvomaseni sustav, metoda koeficijentnog dijagrama, upravljanje omjerom rezonancija

1 INTRODUCTION

Recently, society demands new robot designed to support human. These robots are required to have an ability to accommodate the interaction potential with human operator. In the conventional force control system, several proposed techniques have paid attention to develop force control system and implemented force sensors to detect the external force. However, the force information detected by force sensor has narrow bandwidth due to the soft structure of the strain gauge [1]. To improve the control performance, the sensorless force control technique is proposed to estimate the external force without force sensor. Many research have involved this techniques in order to reduce

the complicity of the overall control system and increase their stability as shown in [2, 3].

In the industrial robot applications, the effects of structural flexibility can lead to limit the performance of a control system [4, 5]. The flexible robot system can be modeled as the two-mass system which consist of a motor and load connected by a spring. Since the actuator is connected to the load side with a transmission mechanism, its elasticity causes resonance in the system. Generally, the conventional PID controller is widely used in the industrial machines and robotics. Although this method offers a simple way to design the controller, it does not perform well when the plant system is unstable or has a resonance structural vibration. Therefore, it is necessary to design the controller that guarantees the robustness and suppresses vibration.

Controlling machine with the mechanical resonance has been receiving increased attention [6]- [7]. A new effective control method, the resonance ratio control [8], has been introduced by Yuki et al. as a new way to guarantee the robustness and suppress the oscillation during task executions for position control system. This method relies on the possibility to change the virtual inertia moment in the motor side by feeding back the estimated reaction torque to the motor in an acceleration dimension. This means that the resonance frequency and the resonance ratio of the system can be changed to an arbitrarily value. In the position control, it is found that the vibration is well compensated by using the resonance ratio gain as $\sqrt{5}$. In addition, the sensorless force servoing based on resonance ratio control was proposed by Katsura [9]. This method has proven itself as an excellent controller for vibration compensation by setting the resonance ratio gain as $\sqrt{6}$.

In this paper, three techniques are proposed for improving the performance of resonance ratio control:

1) A coefficient diagram method (CDM) [10] has been applied to calculate a new gain of the force controller. The CDM method is an algebraic approach combining classical and modern control theories and applied polynomials to represent the system. More reliable parameters selection can be designed based on the stability index and equivalent time constant. From the calculation, a new resonance ratio gain based on the CDM has been presented as 2.0.

2) A multi encoder based disturbance observer (MEDOB) is proposed and applied to estimate the external force on the load side, rather than using the load side disturbance observer (LDOB) [9] or force sensor [4]. The proposed observer is not necessary to estimate the nominal spring coefficient.

3) A new parameter identification is also proposed based upon the LDOB and MEDOB. The correct value of the parameter identification is needed for model based controlling of flexible robot and designation of structural

observer. There are two parameters due to the error in the load side external force estimation of LDOB, which are because of the nominal load mass and the spring parameters. From the experimental setup, it is easy to find the nominal load mass of the system by measuring or finding this value from catalog. By the way, the correct spring coefficient is very difficult to obtain. Analysis of the calculation reveals that the correct region of spring coefficient is found if the response of the load side external force from both LDOB and MEDOB are equal.

From the simulation and experimental results, it is shown that this new identification method, which has the comparison of MEDOB and LDOB, is capable of accurately approximating the spring coefficient. It is also confirm that a new resonance ratio gain as 2.0 is also suitable for suppressing vibration of the mechanical resonance.
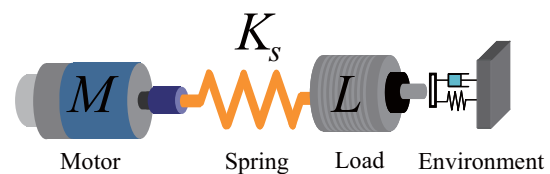

Fig. 1. The model of flexible robot system

2 TWO-MASS SYSTEM MODEL

In recent years, robot systems and intelligent machines have been used not only for industrial processes but also for a wide range of applications. Generally, the mechanics of machine and robot system often consist of a motor M and a load L connected by a flexible structure to transmit the actuator torque to a distant joint as shown in Fig. 1. Since the actuator is connected to the load side with a transmission mechanism, its elasticity causes resonance in the system. Therefore, the elasticity of flexible robot is realized under assumptions that it can be modeled by spring coefficient K_s and mass system. A block diagram of the linear motor with two-mass system that controls under the ideal current source is shown in Fig. 2. The dynamic equation of the linear motor is described by:

$$\ddot{X}_m = -\frac{K_s}{M}X_s + \frac{K_t}{M}I_m, \qquad (1)$$

$$\ddot{X}_l = \frac{K_s}{L}X_s - \frac{1}{L}F_{dl}, \qquad (2)$$

$$\dot{X}_s = \dot{X}_m - \dot{X}_l, \qquad (3)$$

where subscripts m and l denote the motor side and load side, respectively. F_s and F_{dl} are the spring force and the external force on the load side. K_t is the force coefficient, I_m is the current, X_s is the torsional position from the position of the motor X_m and the position of the load X_l,
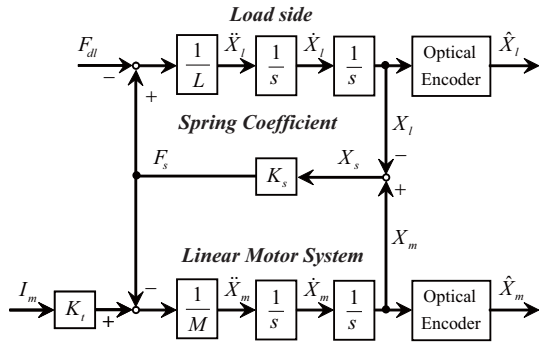
Fig. 2. The block diagram of two-mass system

M and L denote the equivalent mass of the linear motor and load mass, respectively. Naturally, this flexible transmission can negatively affects the overall performance in terms of increased vibrations.

From Fig. 2, the transfer function from current reference I_m to the velocity of motor side $\dot{X}_m$ and the transfer function from current reference I_m to the velocity of load side $\dot{X}_l$ can be calculated as follows

$$\frac{\dot{X}_m}{I_m} = \frac{\frac{K_t}{M}(s^2 + \frac{K_s}{L})}{s^3 + (\frac{K_s}{L} + \frac{K_s}{M})s}, \tag{4}$$

$$\frac{\dot{X}_l}{I_m} = \frac{\frac{K_t K_s}{ML}}{s^3 + (\frac{K_s}{L} + \frac{K_s}{M})s}. \tag{5}$$

Then, the anti-resonance ω_{ar} and resonance frequencies ω_r can be described as follows

$$\omega_r = \sqrt{\frac{K_s}{L} + \frac{K_s}{M}}, \tag{6}$$

$$\omega_{ar} = \sqrt{\frac{K_s}{L}}. \tag{7}$$

3 ESTIMATION OF DISTURBANCE AND EXTERNAL FORCE

3.1 Disturbance Observer

Consequently, a disturbance observer has been used, not only for improving the robustness and bandwidth of the control system, but also for estimation the external force for examples, [11]– [12]. It has been confirmed that a robust force control can be obtained, when a disturbance observer is implemented as the feed forward control for a disturbance force compensation loop. Here, the disturbance force on the motor side F_{dm} is defined as

$$F_{dm} = F_{fm} + D_m \dot{X}_m + F_s + \Delta M \ddot{X}_m + \Delta K_t I_m, \tag{8}$$

where, the resistive force which the direction is opposite to the motor force is the summation of friction force F_{fm},
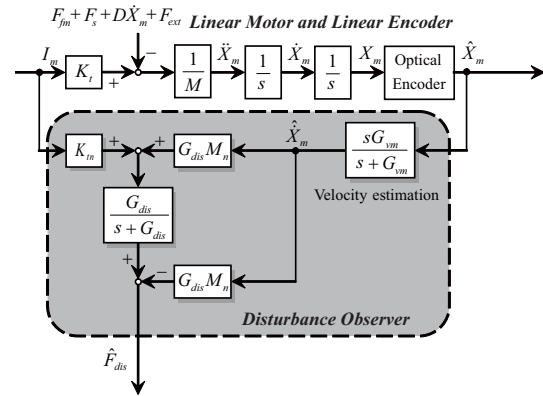

Fig. 3. Disturbance observer

viscous friction $D_m \dot{X}_m$ and the spring force F_s. $\Delta M \ddot{X}_m$ is the variation torque due to changed mass, $\Delta K_t I_m$ is the force ripple due to space harmonics.

In this research, it is assumed that the influence of the friction force is very small by using a small-size of linear motor; thus, the spring force has almost the same value of the disturbance force. Disturbance observer is an external disturbance estimation algorithm that is based upon motor current and velocity information as shown in

$$\hat{F}_{dm} = \frac{G_{dis}}{s + G_{dis}}\Big(K_{tn}I_m + G_{dis}M_n\hat{\dot{X}}_m\Big)$$
$$- G_{dis}M_n\hat{\dot{X}}_m, \tag{9}$$

$$\hat{\dot{X}}_m = \frac{sG_{vm}}{s + G_{vm}}\hat{X}_m, \tag{10}$$

where K_{tn} and M_n are refer to the nominal force coefficient and the nominal motor mass, respectively. G_{dis} is the cut-off frequency of the disturbance observer, G_{vm} is the cut-off frequency of the motor velocity estimation. To apply in the real controller, accurate measured data of velocity is required to provide high accurate force sensing of disturbance observer.

3.2 Load Disturbance Observer

Because of the advantages and unique features of disturbance observer, this approach has received much attention in sensorless force control system. However, instability and vibration of system can occur when using disturbance observer for the two-mass system because of the presence of spring that degrade the overall performance.

To address these problems, a load disturbance observer (LDOB) [9], which is composed of the nominal spring coefficient K_{sn}, the nominal load mass L_n and the load-side encoder, has been proposed as follows
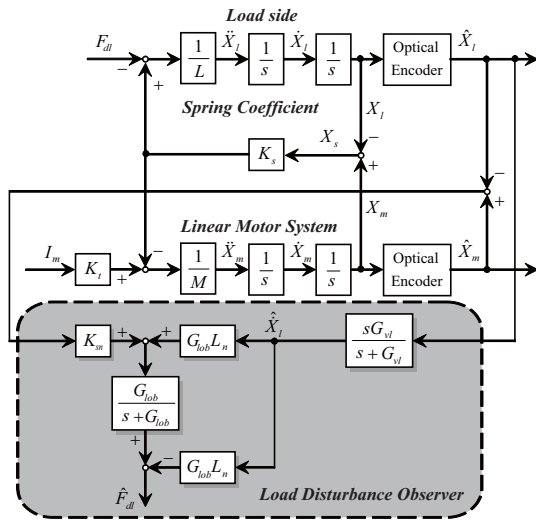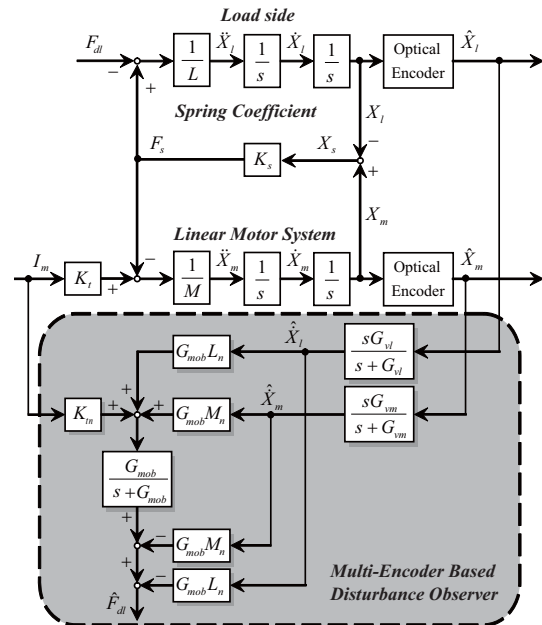
Fig. 4. Load side disturbance observer

Fig. 5. Multi-encoder based disturbance observer

$$F_{dl} = K_s X_s - L_n \ddot{X}_l, \tag{11}$$

$$\hat{F}_{dl} = \left(\frac{G_{lob}}{s + G_{lob}} \Big(K_{sn}(\hat{X}_l - \hat{X}_m) + G_{lob} L_n \hat{\dot{X}}_l \Big) \right.$$
$$\left. - G_{lob} L_n \hat{\dot{X}}_l \right), \tag{12}$$

$$\hat{\dot{X}}_l = \frac{s G_{vl}}{s + G_{vl}} \hat{X}_l, \tag{13}$$

where G_{vl} and G_{lob} are the cut-off frequency of the load velocity estimation and the LDOB, respectively. The structure of LDOB as described in this section can be applied to estimate the external force at the load side as shown in Fig. 4. The LDOB is proposed to estimate the external force on the load side. However, the exact parameters of the spring coefficient is difficult to obtain. Moreover, it can be assumed by a non-linear relationship.

3.3 Multi-Encoder Based Disturbance Observer

In this paper, a novel multi-encoder-based disturbance observer (MEDOB) is proposed for estimating the external force at the load side of flexible robot as shown in Fig. 5. The method to estimate the external force at the load side is obtained from the equation (14), (15) and a simple first-order low-pass filter as follows

$$F_{dl} = K_{tn} I_m - M_n \ddot{X}_m - L_n \ddot{X}_l, \tag{14}$$

$$\hat{F}_{dl} = \left(\frac{G_{mob}}{s + G_{mob}} \Big(K_{tn} I_m + G_{mob} M_n \hat{X}_m \Big) \right.$$
$$\left. + G_{mob} L_n \hat{\dot{X}}_l - G_{mob} M_n \hat{\dot{X}}_m - G_{mob} L_n \hat{\dot{X}}_l \right), \tag{15}$$

where G_{mob} is the cut-off frequency of the MDOB. Compared to the other conventional ways such as state observer [13] and LDOB, the proposed observer based on multi-encoder system offers the advantages of faster response, and high accuracy. By using the proposed observer, it is not necessary to estimate the nominal spring coefficient.

4 CONTROLLER AND IDENTIFICATION

4.1 Resonance Ratio Control Based on Coefficient Diagram Method

A new effective control method, the resonance ratio control, has been introduced by Yuki et al. as a new way to guarantee the robustness and suppress the oscillation during task executions for a torsional vibration in the position control system [8]. Briefly, this approach relies on the possibility to change the virtual inertia moment in the motor side by feeding back the estimated reaction torque to the motor in an acceleration dimension. This means that the resonance frequency and the resonance ratio of the system can be changed to an arbitrarily value. Also, in [9], the resonance control is used in order to achieve the excellent performance that compensates vibration for high-bandwidth force servoing. Due to the compensation of disturbance observer on the motor side, the simplified block diagram of this reaction force feedback is shown in Fig. 6. The controller of robot system consist of a force gain K_p, a velocity gain K_v and a reaction force gain K_r. The feedback force will depend on the force contacted on the robot by a known environment stiffness K_e.
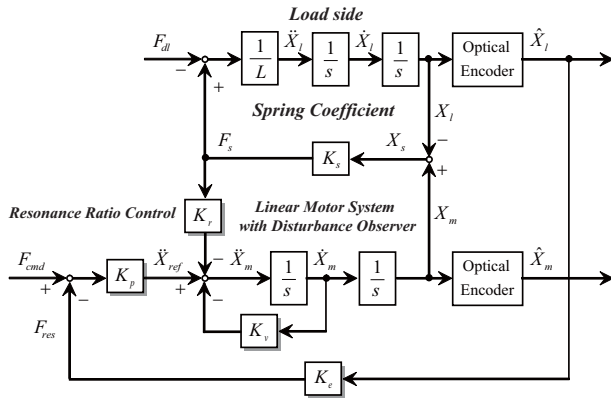
Fig. 6. The simplified block diagram of the resonance ratio control

From Fig. 6, the transfer functions from acceleration reference $\ddot{X}_{ref}$ to motor position $\hat{X}_m$ and motor position $\hat{X}_m$ to load position $\hat{X}_l$ can be calculated as follows

$$\frac{\hat{X}_m}{\ddot{X}_{ref}} = \frac{Ls^2 + K_s}{Ls^4 + K_s(1 + K_r L)s^2}, \quad (16)$$

$$\frac{\hat{X}_l}{\hat{X}_m} = \frac{K_s}{Ls^2 + K_s}. \quad (17)$$

Such a reaction force feedback is able to change the resonance frequency of the system. The new anti-resonance frequency ω_{ar} and the new resonance frequency ω_r of the system can be computed as follows

$$\omega_r = \sqrt{\frac{K_s}{L}(1 + K_r L)}, \quad (18)$$

$$\omega_{ar} = \sqrt{\frac{K_s}{L}}. \quad (19)$$

The transfer function of the force servoing based on resonance ratio control is given by

$$\frac{F_{res}}{F_{cmd}} = \frac{K_p K_e \omega_{ar}^2}{s^4 + K_v s^3 + \omega_r^2 s^2 + K_v \omega_{ar}^2 s + K_p K_e \omega_{ar}^2}. \quad (20)$$

In the conventional controller design, the control system is realized as the critically damped system. When the damping ratio is equal to 1, the roots of the characteristic equation are real and identical [9]. Each control gains are given as follows

$$K_v = K_{vk} = 4\omega_{ar}, \quad (21)$$

$$K_p = K_{pk} = \frac{\omega_{ar}^2}{K_e}, \quad (22)$$

$$K = K_k = \frac{\omega_r}{\omega_{ar}} = \sqrt{6}, \quad (23)$$

$$K_r = K_{rk} = \frac{5}{L_1}. \quad (24)$$

By setting these designed gains, the resonance ratio is chosen to be $\sqrt{6}$. Therefore, the force response exhibits no overshoot and vibration. In this paper, a new resonance ratio parameter is calculated by using the coefficient diagram method (CDM). The CDM design method is used to design the characteristic polynomial of the closed loop system by achieving a good balance of stability and good robust performance. As it is seen from equation (20), the coefficients of characteristic polynomial a_i are found as

$$a_0 = K_p K_e \omega_{ar}^2, \quad (25)$$

$$a_1 = K_v \omega_{ar}^2, \quad (26)$$

$$a_2 = \omega_r^2, \quad (27)$$

$$a_3 = K_v, \quad (28)$$

$$a_4 = 1.0. \quad (29)$$

The standard stability indices γ_i for the Manabe form are chosen as γ_1=2.5, γ_2=2.0, and γ_3=2.0.

$$\tau = \frac{a_1}{a_0} = \frac{K_v}{K_p K_e} \quad (30)$$

$$\gamma_1 = \frac{a_1^2}{a_0 a_2} = \frac{K_v^2 \omega_{ar}^2}{K_p K_e \omega_r^2} = 2.5 \quad (31)$$

$$\gamma_2 = \frac{a_2^2}{a_1 a_3} = \frac{\omega_r^4}{K_v^2 \omega_{ar}^2} = 2.0 \quad (32)$$

$$\gamma_3 = \frac{a_3^2}{a_2 a_4} = \frac{K_v^2}{\omega_r^2} = 2.0 \quad (33)$$

Thus, the controller parameters calculated by the design of CDM are given as follows

$$K_v = K_{vc} = \sqrt{2}\omega_r, \quad (34)$$

$$K_p = K_{pc} = \frac{4\omega_{ar}^2}{5K_e}, \quad (35)$$

$$K = K_c = \frac{\omega_r}{\omega_{ar}} = 2.0, \quad (36)$$

$$K_r = K_{rc} = \frac{3}{L_1}. \quad (37)$$

By setting these controller gain, a new resonance ratio parameter is chosen as 2.0.

4.2 Feedforward Load Disturbance Compensation

The block diagram of the proposed control structure is shown in Fig. 7. A robust motion control of each motor has been achieved by feedback the inner disturbance observer loop. By using the divider's gain $1/K_{tn}$, the disturbance force is transformed to the compensation current $\hat{I}_{dis}$, and it is utilized to cancel out the disturbance on the motor side and the uncertainty of a system due to the parameter variation.

The load disturbance compensation is introduced to compute and feedback the estimated load disturbance force
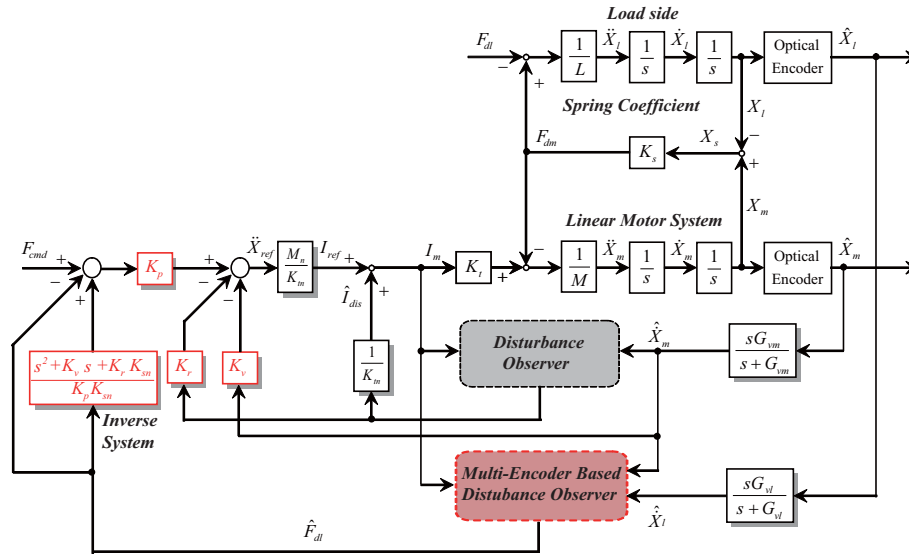
Fig. 7. The resonance ratio control based on MEDOB and CDM

through the inverse system of the motor side. The inverse system can be represented by the transfer function from F_{cmd} to F_{res} as shown in (20) and from F_{dl} to F_{res} as follows

$$\frac{F_{res}}{F_{dl}} = \frac{\frac{1}{L}K_e(s^2 + K_v s + K_r K_s)}{s^4 + K_v s^3 + \omega_r^2 s^2 + K_v \omega_{ar}^2 s + K_p K_e \omega_{ar}^2}. \tag{38}$$

Then, the inverse system can be calculated by the following equation:

$$\frac{F_{cmd}}{F_{dl}} = \frac{s^2 + K_v s + K_r K_s}{K_p K_s}. \tag{39}$$

In the next section, the experiment and simulation examples illustrate that the CDM design method gives significantly improved performance both for a step input force command and for vibration suppression.

4.3 Parameter Identification Based on LDOB and MEDOB

The correct value of the parameter identification of spring coefficient is needed for model based controlling of resonance ratio and designation of structural observer as well. The main contribution of this paper is that, using the proposed parameter identification, the correct spring coefficient is obtained, improving for the performance of resonant ratio control. Figure 8 shows the proposed identification method, where the sinusoidal signal is fed as the force reference and the ramp signal is used to vary the spring coefficient of the LDOB. The sinusoidal signal used for the

parameter identification is designed by the following equation:

$$u(kT_s) = A_0 + w(k)sin(w_k kT_s), \quad 0 \le k \le N - 1, \tag{40}$$

$$w(k) = Asat(k/0.1N)sat((N-k)/0.1N), \tag{41}$$

$$w_k = w_{start} + \frac{k}{N}(w_{end} - w_{start}), \tag{42}$$

where, $w(k)$ is a weighting or window function that causes the input to start at zero, ramp up to amplitude A, and ramp down to zero at the end. The "sat" is the saturation function, which is linear from -1 to +1 and saturates at -1 for arguments less than -1 and at +1 for arguments greater that +1. The constant A_0 is an offset value added to make the input have zero average value. Sampling time for command generation and total points of command signal are represented by T_s and N, respectively.

The comparison of load side external force is used to identify a correct region of the spring coefficient. According to the structural of the observers, if the load side external force error between LDOB and MEDOB is nearly zero, then the correct region of spring coefficient is found.

5 SIMULATION RESULTS

5.1 Simulation Results of the Proposed Identification Method

Numerical simulations are given to confirm the validity of the proposed parameter identification. The correct stiffness coefficient K_s was set as 1000 N/m. The comparison result of the load side external force of LDOB and
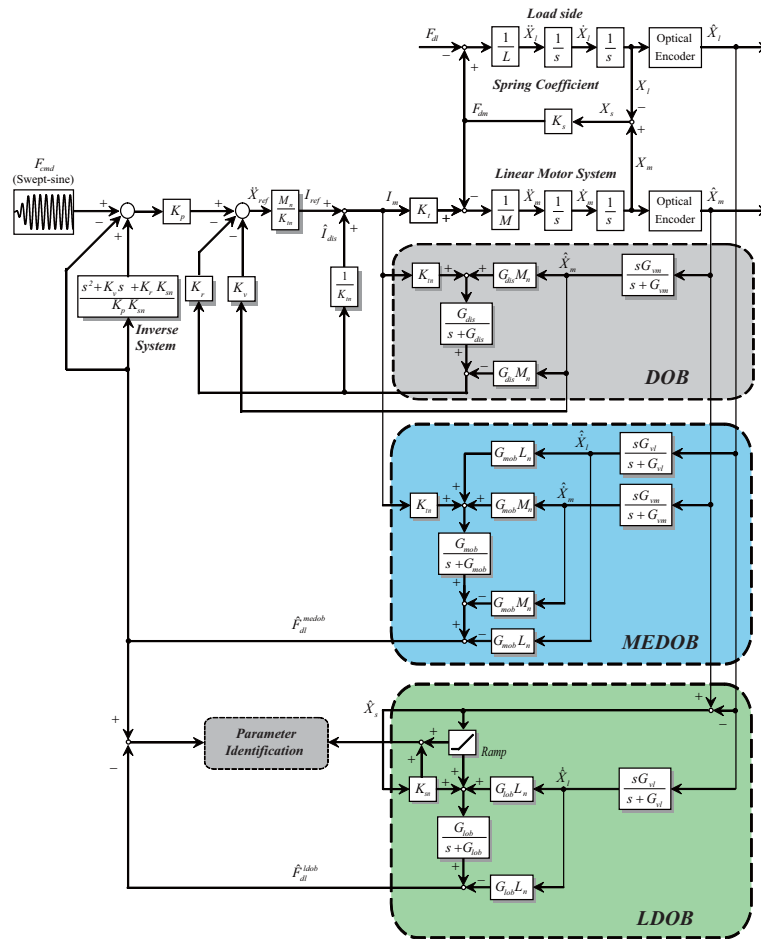
Fig. 8. The resonance ratio control with the proposed parameter identification

MEDOB is shown in Fig. 9. The variation of the nominal stiffness coefficient K_{sn} was bounded from 950 N/m to 1050 N/m. It can be seen from 0 s to 4 s that the amplitude of the load side external force of LDOB is lower than MEDOB in the case of $K_{sn} < K_s$. By reaching the correct region of the spring coefficient at 5 s, the load side external force from LDOB can be tracked almost identically over the load side external force from MEDOB as shown in Fig. 9 (b) and (c). It is seen from results that adding too much stiffness parameter $K_{sn} > K_s$ give a poor response with very large amplitude of the load side external force estimation. Thus, at 5 s, the correct stiffness coefficient can be found as 1000 N/m.

5.2 Simulation Results of the Proposed Resonance Ratio Control

Numerical simulations are given to confirm the validity of the proposed approach. The results obtained from the proposed approach is compared with the results obtained from the conventional resonance ratio control and

without the reaction force feedback. The comparison of the bode diagram with resonance ratio control is shown Fig. 10. From the result, the lowest order with the higher bandwidth and no-overshoot are obtained. In the simulation results, the force command input is a step function with the magnitude of 4.0 N. It is seen from Fig. 11 that without reaction force feedback give a poor response with a very large vibration. On the other hand, the vibration are well compensated in the both case of the resonance ratio control. It is clear from these results that the resonance ratio control based on CDM design approach gives a good response with no overshoot and short settling time compared to the conventional method.

6 EXPERIMENTAL RESULTS

The experimental setup of the flexible robot consists of the linear motors, linear guide devices, spring, two encoders at the motor and load side as shown in Fig. 12. The robot system is controlled by a PC using RT-Linux with a sampling time of 100 μs. The computer is equipped
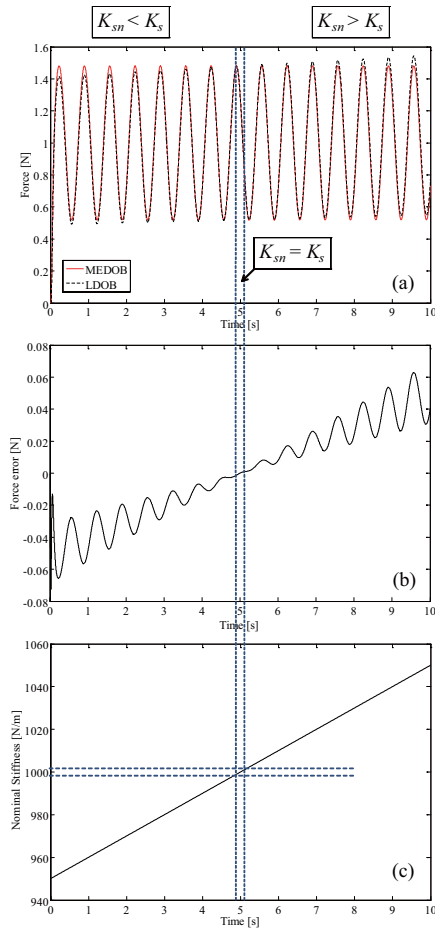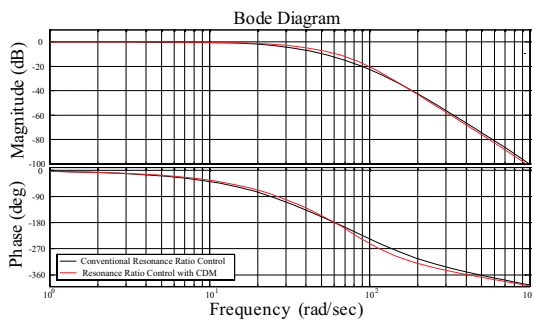
Fig. 9. The simulation results

Fig. 10. Bode diagram

with analog output board, analog input board, and encoder-pulse counter board. All of the data from sensors as well as the controllers are written in the C language. The specifications of the linear motor and the parameters used in the experiments are shown in Table 1.
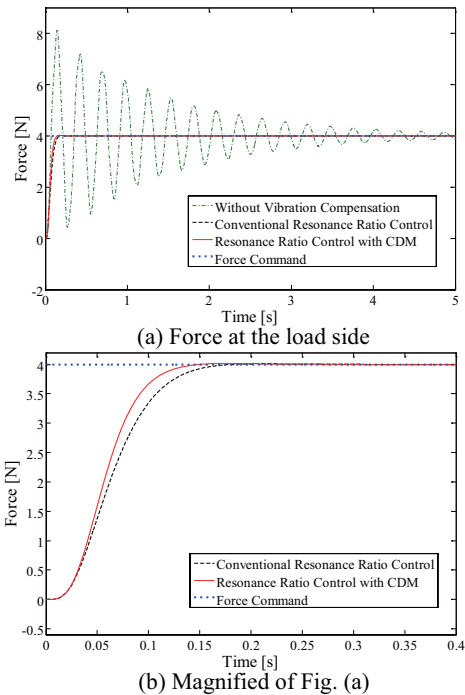

(a) Force at the load side

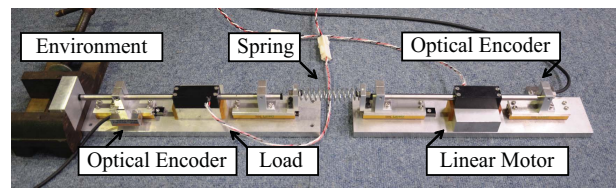(b) Magnified of Fig. (a)

Fig. 11. The simulation results

Fig. 12. The experimental setup of the flexible robot system

Table 1. Parameters used in experimental setup

Mass of motor	M	0.245 kg
Force constant	K_t	3.333
Load	M	0.245 kg
Spring coefficient	K_{sn}	1100 N/m
Force gain	K_{pk}, K_{pc}	4.49, 3.59
Velocity gain	K_{vk}, K_{vc}	268.02, 189.52
Reaction force gain	K_{rk}, K_{rc}	20.41, 12.24
Resonance ratio gain	K_k, K_c	$\sqrt{6}$, 2
Cut-off freq. of vel.	G_{ve}	1000 rad/s
Cut-off freq. of DOB	G_{dis}	1000 rad/s
Cut-off freq. of LDOB	G_{lob}	800 rad/s
Cut-off freq. of MEDOB	G_{mob}	800 rad/s

6.1 Experimental Results of the Proposed Identification Method

Three classes of experiment was performed to identify the region of correct value of stiffness coefficient. Exper-
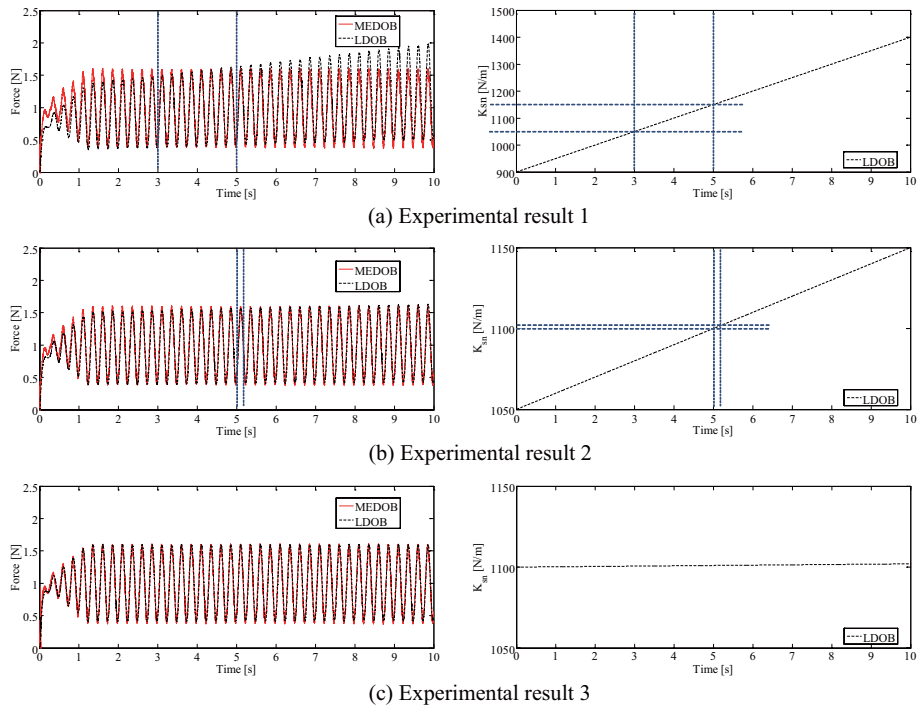
(a) Experimental result 1

(b) Experimental result 2

(c) Experimental result 3

Fig. 13. The experimental results

iments of contact motion are investigated. In this experiment, a hard environment, which is an aluminum block, was used.

First, we performed experiments with varying of the wide range of the nominal stiffness coefficient; the nominal stiffness coefficient is set to increase from $900\ N/m$ to $1400\ N/m$. Figure 13 (a) show the comparison of the load side external force between LDOB and MEDOB. From the experimental results, the improvement in the load side external force estimation of LDOB are illustrated at 3.0-5.0s. Therefore, the region of the correct value of K_{sn} are bounded from $1050N/m$ to $1150N/m$, while providing only a rough estimate of parameters. In the second experiment, the nominal stiffness coefficient is set to increase from $1050\ N/m$ to $1150\ N/m$. The estimation performance of LDOB is more improving than that of the previous experiment since the correct value of spring coefficient is applied in the observer. From the experimental result in Fig. 13 (b), the force peak of LDOB is over than the MEDOB in the interval time at 5.2 s. An increase of the nominal stiffness coefficient produced the amplitude error enlargement of the load side external force estimation. Therefore, we acquired the correct region of the nominal stiffness coefficient as $1100\ N/m$. When the nominal stiffness coefficient at $1100\ N/m$ is utilized in the LDOB as shown in Fig. 13 (c), we found that the external force response of the LDOB is almost equal to the MEDOB. By

using the proposed parameter identification, it is possible to identify parameters with a very few experiment.

6.2 Experimental Results of the Proposed Resonance Ratio Control

The experiment was performed to evaluate the performance of the proposed approach with the input step function. All of the identified parameters as shown in the previous section was used to calculate the controller gain. A flexible robot system is moved to contact the aluminum block.

The controller without the reaction force feedback compensation was chosen to illustrate the worst-case vibration. Figures 14 (a) and (b) show the force response at the load side and motor side, respectively. Without the vibration compensation, it is found that the response of force and position are oscillated as shown in Fig. 14 (b) and (d). The influence of the reaction force feedback can be observed to significantly reduced the effective vibration by using the resonance ratio control. The experimented response also shows a good correlation with the simulation results. The improvement in the position and velocity responses at the motor side and load side are illustrated in Fig. 15. By using the proposed resonance ratio control based on the CDM, the best results for the faster response without overshoot is obtained. The vibration on the system can be rejected very successfully. Moreover, the time
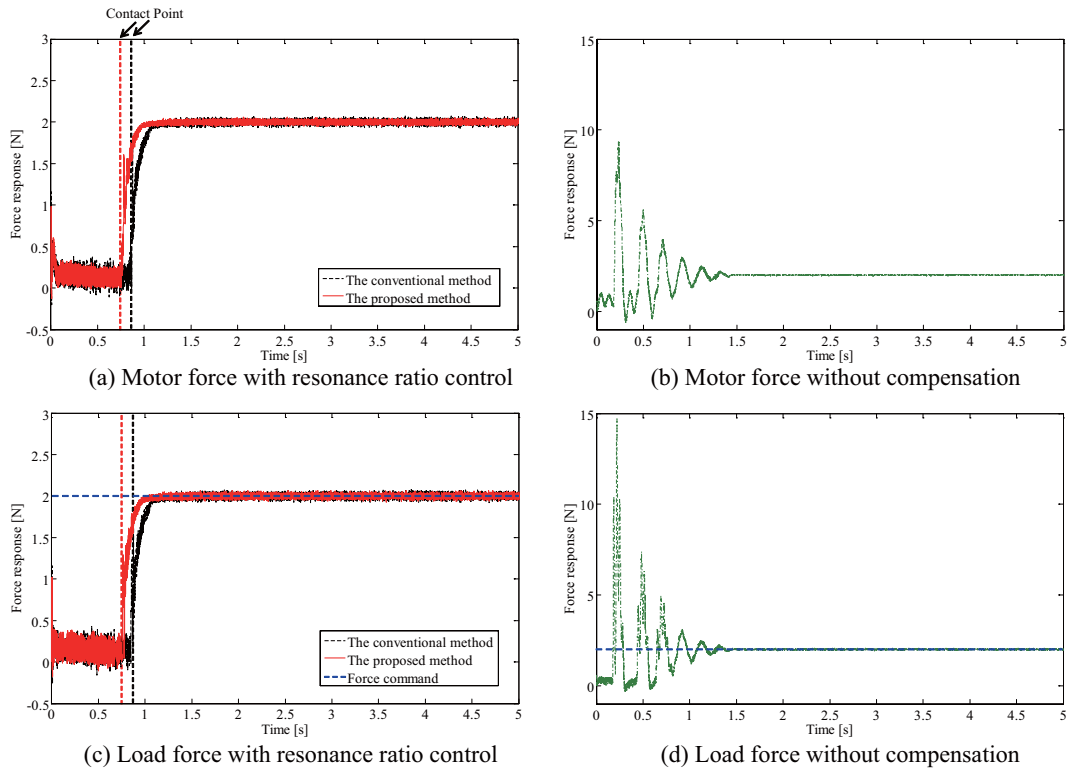
(a) Motor force with resonance ratio control

(b) Motor force without compensation

(c) Load force with resonance ratio control

(d) Load force without compensation

Fig. 14. The force response of the flexible robot system

(a) Motor position

(b) Motor velocity

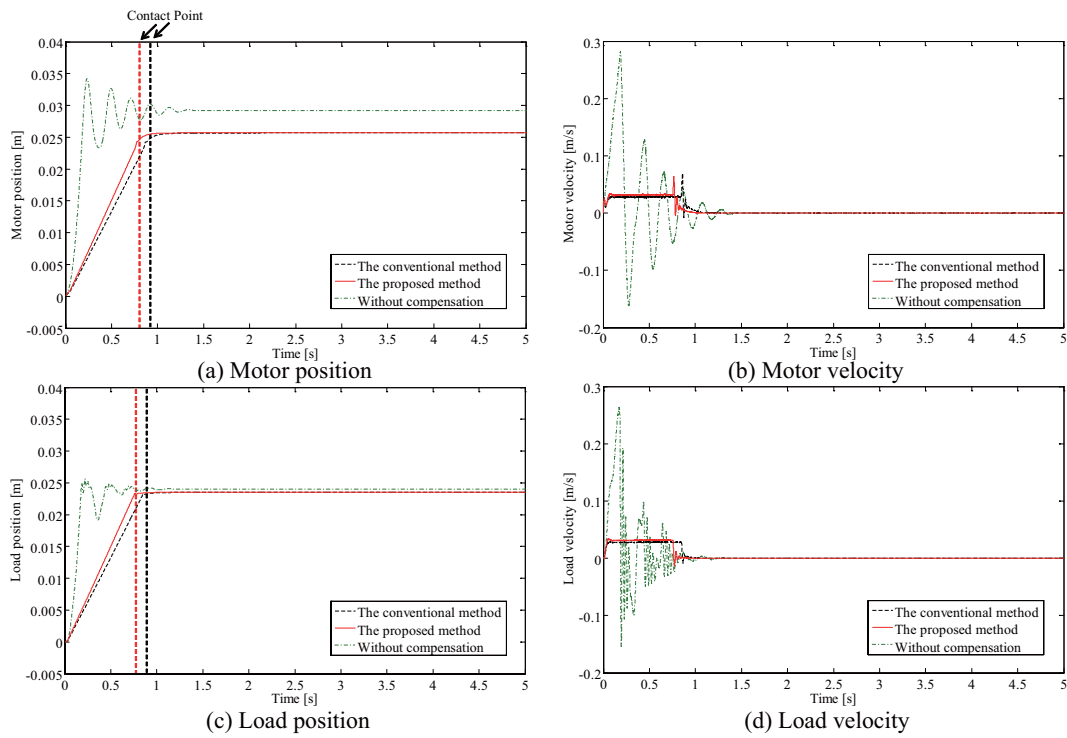(c) Load position

(d) Load velocity

Fig. 15. The motion movements of the flexible robot system

response of the controlled closed loop system has a small settling time and the system is high robustness against the parameter variations and disturbance effects.

7   CONCLUSION

In this paper, a new resonance ratio gain has been presented as 2.0 for the rejection of vibration in the flexible robot system. The proposed gain controller based on the CDM is simple to design and easily implemented into the resonance ratio control. By using the proposed controller design based on CDM method, the best results for the fast response and vibration suppression in the flexible robot system are also achieved. Current work also includes the design of the MEDOB to estimate the external force on the load side. No feedback force sensors are required in the system. By using the proposed MEDOB, it is not necessary to estimate the nominal spring coefficient.

A new parameter identification has been presented for the consideration of the correct value of stiffness coefficient in the resonant ratio control. The proposed identification based on the LDOB and MEODB is simple to design and easily implemented into the system. Analysis of the calculation reveals that the correct region of spring coefficient is bounded if the differentiation of load side external force between both LDOB and MEDOB is zero. From the experimental and simulation results, the correct value of stiffness coefficient is obtained and the load side external force from LDOB can be tracked almost identically over the load side external force from MEDOB. These results serve as guidelines to identify the stiffness of the unknown environment parameters. For future works, it might be useful to apply and develop a model of environment for haptic technology, advanced medical device and telerobotic research.

REFERENCES

[1] S. Katsura, Y. Matsumoto, and K. Ohnishi, "Modeling of force sensing and validation of disturbance observer for force control," *IEEE Trans. Ind. Electron.*, vol. 54, no. 1, pp. 530–538, 2007.

[2] Islam, S. M. Khalil, and A. Şabanoviç, *Sensorless torque/force control.* Croatia: InTech, 2011.

[3] W. Iida and K. Ohnishi, "Sensorless force control with force error observer," in *Proceedings in The IEEE International Conference on Industrial Technology, ICIT'2003*, (Maribor, Slovenia), pp. 157–162, December 2003.

[4] G. Ferretti, G. Magnani, and P. Rocco, "Impedance control for elastic joints industrial manipulators," *IEEE Trans. Robot. Autom.*, vol. 20, no. 3, pp. 488–498, 2004.

[5] A. Hace, K. Jezernik, and A. Sabanovic, "Smc with disturbance observer for a linear belt drive," *IEEE Trans. Ind. Electron.*, vol. 54, no. 6, pp. 3402–3412, 2007.

[6] E. Pereira, S. Aphale, V. Feliu, and S. Moheimani, "Integral resonant control for vibration damping and precise tip-positioning of a single-link flexible manipulator," *IEEE Trans. Mechatron.*, vol. 16, no. 2, pp. 232–240, 2007.

[7] C. Mitsantisuk, K. Ohishi, and S. Katsura, "Resonance ratio control based on coefficient diagram method for force control of flexible robot system," in *Proceedings in The 12th International Workshop on Advanced Motion Control, AMC'2012*, (Sarajevo, Bosnia and Herzegovina), pp. 1–6, March 2012.

[8] K. Yuki, T. Murakami, and K. Ohnishi, "Vibration control of 2 mass resonant system by resonant ratio control," in *Proceedings in The International Conference on Industrial Electronics, Control, and Instrumentation, IECON'1993*, (Lahaina, Hawaii), pp. 2009–2014, November 1993.

[9] S. Katsura, J. Suzuki, and K. Ohnishi, "Pushing operation by flexible manipulator taking environmental information into account," *IEEE Trans. Ind. Electron.*, vol. 53, no. 53, pp. 1688–1697, 2006.

[10] S. Manabe, "The coefficient diagram method," in *Proceedings in The 4th IFAC Symposium on Automatic Cont. in Aerospace.*, (Seoul, Korea), pp. 199–210, August 1998.

[11] K. Ohishi, K. Ohnishi, and K. Miyachi, "Torque-speed regulation of dc motor based on load torque estimation," in *Proceedings in The IEEJ IPEC*, (Tokyo, Japan), pp. 1209–1216, March 1983.

[12] J. Back and H. Shim, "Adding robustness to nominal output feedback controllers for uncertain nonlinear systems: A nonlinear version of disturbance observer," *AUTOMATIKA*, vol. 44, no. 10, pp. 2528–2537, 2008.

[13] Y. Ohba, M. Sazawa, K. Ohishi, T. Asai, K. Majima, Y. Yoshizawa, and K. Kageyam, "Sensorless force control for injection molding machine using reaction torque observer considering torsion phenomena," *IEEE Trans. Ind. Electron.*, vol. 56, no. 81, pp. 2955–2960, 2009.

Chowarit Mitsantisuk received the B. Eng. degree in electrical engineering from Thammasat University, Pathumthani, Thailand, in 2004, and the M. Eng. degree in Electrical, Electronics and Information Engineering and D. Eng. degree in energy and environment science from the Nagaoka University of Technology, Japan, in 2007 and 2010, respectively.

From 2010 to 2012, he was also a Postdoctoral Fellow of the Japan Society for the Promotion of Science with Nagaoka University of Technology. Since 2012, he has been with the Department of Electrical Engineering, Kasetsart University, Thailand. His research interests include motion control, force control, human-robot interaction, sensor fusion, advanced medical device and real-world haptics.

Dr. Chowarit is a Member of the IEEE Industrial Electronics Society. He was the recipient of the IEEE Student Scholarship Award at the 2009 IEEE International Conference on Industrial Electronics, Control, and Instrumentation from the IEEE Industrial Electronics Society.

Manuel Nandayapa received a B.S. degree in Electronics Engineering from Institute of Technology of Tuxtla Gutierrez, Chiapas, Mexico in 1997, M.S. degree in Mechatronics Engineering from CENIDET, Morelos, Mexico in 2003, and D.Eng degree in energy and environmental science from the Nagaoka University of Technology, Japan, in 2012. His research interests include mechatronics, and motion control and he is with the Department of Industrial and Manufacturing Engineering at Autonomous University of Ciudad Juarez. Dr. Nandayapa is Member of the IEEE Industrial Electronics Society and Robotics Automation Society, the Institute of Electrical Engineers of Japan (IEEJ), and Robotics Society of Japan (RSJ).

Kiyoshi Ohishi received the B.E., M.E., and Ph.D. degrees in electrical engineering from Keio University, Yokohama, Japan, in 1981, 1983, and 1986, respectively.

From 1986 to 1993, he was an Associate Professor with the Osaka Institute of Technology, Osaka, Japan. Since 1993, he has been with the Department of Electrical Engineering, Nagaoka University of Technology, Nagaoka, Japan, where he became a Professor in 2003. His research interests include power electronics, mechatronics, and motion control.

Dr. Ohishi was the recipient of the Outstanding Paper Awards at the 1985 IEEE International Conference on Industrial Electronics, Control, and Instrumentation (IECON) and the Best Paper Awards at IECON 2002, IECON 2004 from the IEEE Industrial Electronics Society. He was also the recipient of the Best Paper Award from the Institute of Electrical Engineers of Japan in 2002.

Seiichiro Katsura received the B.E. degree in system design engineering and the M.E. and Ph.D. degrees in integrated design engineering from Keio University, Yokohama, Japan, in 2001, 2002 and 2004, respectively.

From 2004 to 2005, he was also a Postdoctoral Fellow with Keio University. From 2005 to 2008, he was with Nagaoka University of Technology, Nagaoka, Japan. Since 2008, he has been with the Department of System Design Engineering, Keio University. His research interests include real-world haptics, human support space, systems energy conversion, and electromechanical integration systems.

Dr. Katsura was a Research Fellow of the Japan Society for the Promotion of Science from 2003 to 2005. He was the recipient of the Best Paper Awards from the Institute of Electrical Engineers of Japan in 2003, the Dr. Yasujiro Niwa Outstanding Paper Award in 2004, and the 2008 European Power Electronics and Drives-Power Electronics and Motion Control Conference Best Paper Award.

AUTHORS' ADDRESSES

Dr. Chowarit Mitsantisuk, D. Eng.
Department of Electrical Engineering,
Kasetsart University,
50 Phaholyothin Rd., Ladyao, Jatujak, Bangkok, 10900,
Thailand
e-mail: chowarit.ku@gmail.com, fengcrm@ku.ac.th
Dr. Manuel Nandayapa, D. Eng.
Department of Industrial and Manufacturing Engineering,
Autonomous University of Ciudad Juarez,
Ave. del Charro 450 Norte, C.P. 32310. Cd. Juarez,
Chihuahua, Mexico
e-mail:mnandaya@uacj.mx, mnandayapa@ieee.org
Prof. Kiyoshi Ohishi, Ph. D.
Department of Electrical Engineering,
Nagaoka University of Technology,
1603-1, Kamitomiokamachi, Nagaoka, Niigata, 940-2188,
Japan
e-mail: ohishi@vos.nagaokaut.ac.jp
Assoc. Prof. Seiichiro Katsura, Ph. D.
Department of System Design Engineering,
Keio University,
3-14-1 Hiyoshi, Kouhoku-Ku, Yokohama, Kanagawa, Japan
e-mail: katsura@sd.keio.ac.jp